Exploration of charge-transfer exciton formation in organic semiconductors through transient photoconductivity measurements

Afina Neunzert

Mentor: Oksana Ostroverkhova

June 3, 2013

Abstract

This project investigated transient photoconductivity in organic donor-acceptor (D-A) systems, where a flourinated anthradithiophene, ADT-TES-F, acts as the donor. Various acceptor molecules were used, with different sidegroups, and different HOMO (highest occupied molecular orbital) and LUMO (lowest unoccupied molecular orbital) energy level offsets relative to the acceptor. Thin film composites of donor and acceptor materials were excited with sub-nanosecond 355 nm laser pulses, and the photoconductivity of the sample was measured up to several microseconds after excitation. Comparing the response of acceptor molecules with different packing properties and energy level offsets allowed insight into the generation and dynamics of charge carriers in the sample, including the formation of CT (charge-transfer) excitons. In pristine films and in samples with a small donor-acceptor spatial separation, the primary contribution to the peak photocurrent was simply the dissociation of a precursor state to the donor exciton. In systems where the spatial separation was greater, CT exciton formation dominated charge carrier generation at low E-fields. There was up to a factor of two increase in the efficiency of charge carrier generation in these samples due to CT exciton dissociation. When higher electric fields were applied, fast charge carrier generation dominated and the presence of the acceptor did not lead to an improvement in charge carrier generation efficiency.

These results allow us to infer the following picture of charge carrier dynamics within the sample. When the excitation pulse hits the sample, a precursor state is formed, which in pristine samples, gives rise to a donor exciton and fast generation of charge carriers. In D-A systems, however, there is a competition process between the formation of donor excitons and charge transfer (CT) exciton states. CT exciton formation is followed by a relatively slow process of charge carrier generation via exciton dissociation. In systems with a large D-A separation, this CT state is more likely to make an important contribution to the photoconductivity, because it dissociates more easily.

Acknowledgements

Thanks are due to Mark Kendrick, with whom I worked on this project, and whose explanations of both the underlying physics and the experimental procedure were integral to my ability to write this thesis; to Oksana Ostroverkhova, who has been a mentor to me for most of my undergraduate education, and who always has encouraged and helped me to achieve at the highest level possible; to all other members of the research group with whom I have worked, for answering my constant questions and providing a supportive environment; and finally to my peers in the PH403 thesis course for valuable edits on this document itself.

Contents

List of Figures

1 Introduction

1.1 Motivation and summary

Organic semiconductors have drawn significant research interest in recent years because they represent new avenues of development for a wide range of applications, including photovoltaics, display, and sensing technology. [2] Of particular interest is the fact that they are tunable: different molecules can be synthesized and combined to form donor-acceptor (D-A) systems with properties unique to the combination. Organic semiconductors are also solution generally solution processable and easy to fabricate, which makes them useful alternatives to inorganic semiconductors despite their lower power conversion efficiencies. [1]

Our goal for this project was to examine a variety of D-A systems with different acceptors, to determine how the properties of the acceptor molecules (including their sidegroups and HOMO/LUMO energy levels) affected transient photoconductivy, and to use that information to synthesize a picture of charge carrier dynamics within the sample. By understanding how the properties of the acceptor molecules influence the generation and recombination of charge carriers, we can provide information to guide new applications for these materials.

Transient photoconductivity is an important experimental technique for studying these materials because it allows us to probe the samples on timescales of nanoseconds to microseconds. In this project we mixed donor and acceptor molecules in solution, deposited them on electrodes, applied a voltage across the sample, and excited it with a sub-nanosecond-duration laser pulse. Then we measured the resulting current as a function of time. From the shapes of the rise times and decays, we were able to obtain information about the population of free charge carriers present in the system shortly after excitation. By comparing the trends under different electric field strengths, we were able to obtain information about the kinds of states those charge carriers were in.

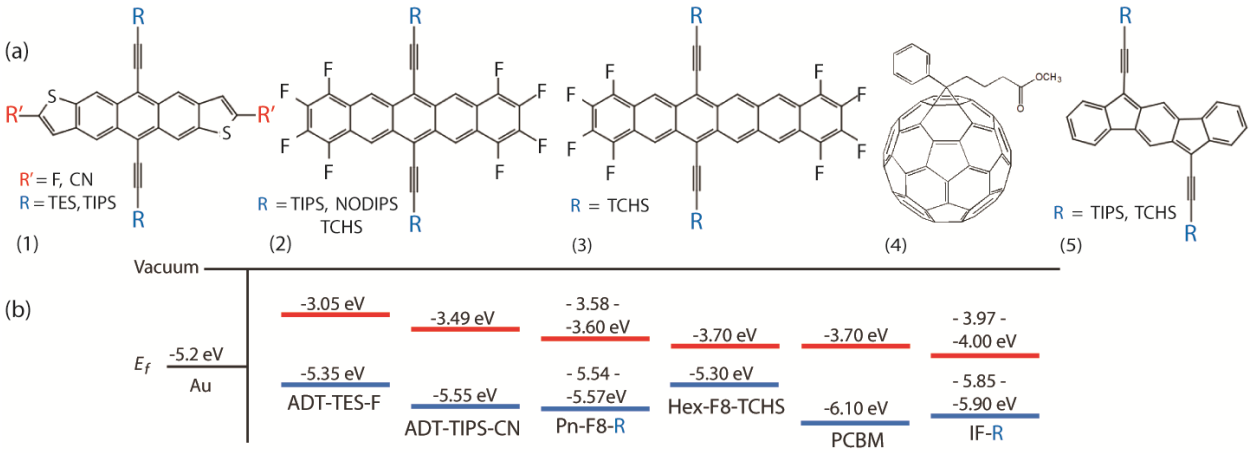

Figure 1: Molecular structure diagrams and energy levels for the materials studied. The donor (ADT-TES-F, where R=TES and R'=F) is shown in (a.1). The acceptors were as follows: ADT-TIPS-CN (also a.1, with R=TIPS and R'=CN), pentacene (Pn) derivatives (a.2), hexacene (Hex) derivatives (a.3), PCBM (a.4), and indenofluorine (IF) derivatives (a.4). The HOMO and LUMO energies of each are shown in (b), in comparison with the gold electrodes and the vacuum energy. Figure from [3].

1.2 A note on the content of this document

This thesis is primarily experimental in nature, but will also cover some theoretical background. It aims to provide the reader with an introduction to transient photoconductivity at a level suitable for an undergraduate student unfamiliar with the subject. Also, it may be a useful reference for new users of the transient photoconductivity experimental setup in our lab. To that end, the experimental methods section is supplemented by two appendices: a calibration guide, and a short description of recent updates to the experimental setup described in the body of the thesis.

1.3 Choice of samples

Anthradithiophene (ADT) derivatives are promising candidates for use in photovoltaics and other applications because they have relatively high charge carrier mobilities and high photoconductive gains. We used ADT-TES-F as the donor for all of our composites. This molecule consists of an anthradithiophene backbone with endgroups and sidegroups attached, as shown in figure 1. The sidegroups (TES, in this case; others are shown in figure 2) influence molec-

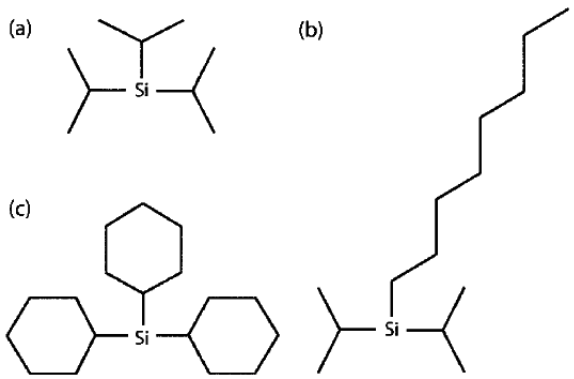

Figure 2: Sidegroup structures (shown as R groups in figure 1). Show here are (a) TIPS, (b) NODIPS, and (c) TCHS.

ular packing properties and in turn the movement of charge carriers through the material.

The acceptors studied were a more widely varied group, including another anthradithiophene derivative (ADT-TIPS-CN), pentacene and hexacene derivatives. The variety was chosen to shed light on the effects of both packing, and the energy gap between the highest occupied molecular orbital (HOMO) and the lowest unoccupied molecular orbital (LUMO) within each molecule. Packing and energy level offsets have been identified as major factors in determining the optical band gap and charge carrier dynamics in organic semiconductors. [1]

The D-A systems used in this study were of a type known as bulk heterojunctions (BHJs). BHJs are distinct from bilayer systems in that the donor and acceptor are blended in the device's active layer, rather than forming two different regions. The use of BHJs has helped to overcome the issue of short exciton difficusion length in organic semiconductors (although this is a larger problem for polymers, it remains an important issue even for small-molecule materials such as the ones we studied). [1] The samples studied were thin ($\lesssim 1\mu$m) films containing a mixture of donor and acceptor molecules, prepared in solution and deposited as drop-cast films on electrodes.

2 Transient photoconductivity theory

The following is a brief and minimally technical discussion of the phenomenon of transient photoconductivity. It is largely based on [3, 1].

1. The material is hit with a pulse of light. Electrons are excited from the ground state (the highest occupied molecular orbital, or HOMO level) to a higher state (typically the lowest unoccupied molecular orbital, or LUMO level). Electrons leave behind holes, which act as positive charge carriers, in their place. As long as charge carriers remain free to move, current will flow across the sample in the presence of an externally applied electric field.

2. However, the excited state created by the pulse of light is generally short-lived. There are a variety of different things that can happen after this point. The possibilities include:

   (a) The electron and hole dissociate and are free to be conducted through the sample (increases the photocurrent).

   (b) The electron and hole recombine, and no free charge carrier results (does not increase the photocurrent).

   (c) The Coulomb attraction between the negatively charged electron and the positively charged hole lead cause to form a bound state called an exciton. The exciton may dissociate under an electric field, or the electron and hole may recombine as in case (b). Because the electron and hole remain with the donor molecule, this is known as a donor exciton.

   (d) The electron and hole become localized on different molecules (a process facilitated by an acceptor with a lower LUMO level than the donor, so that the transition is energetically favorable), and form a bound state. This is known as

a charge-transfer (CT) exciton. CT exciton formation is diagrammed in figure 3 and discussed in more detail in the following section.

3. The initial excitation, and the subsequent processes of step (2), lead to a population of free charge carriers within the sample. Under the application of an electric field, the charge carriers move, forming a current. This is a photocurrent: a current produced specifically by the excitation of the material by light. The photocurrent rises from zero to some peak value immediately after the excitation pulse (meaning that the total current rises from its background, or dark current, to a peak). The rise time in the samples we studied was generally on the order of 1 ns or shorter. The application of a higher electric field typically leads to higher photocurrents, as the electric field assists in separating electrons and holes. It can also influence the shape of the photocurrent rise and decay curves.

4. As the charge carriers move, they may recombine or be trapped. Trapping occurs when defects in the sample cause an energy level between the valence and conduction band to become accessible. A charge carrier which moves to this energy level may become "trapped", preventing it from contributing to the current flow.

5. After the excitation pulse ends, the processes of recombination, trapping, and charge carrier motion continue. This causes the photocurrent to decay, albeit on a slower timescale than the initial rise. Decay takes place on the order of a few microseconds. The "transient" part of the term "transient photoconductivity" refers to this timescale. ("Transient" being opposed to continuous-wave photoconductivity, where the excitation is constant and the photocurrent does not have a chance to decay.)

2.1 Charge-transfer excitons

The following material is based largely on [5].

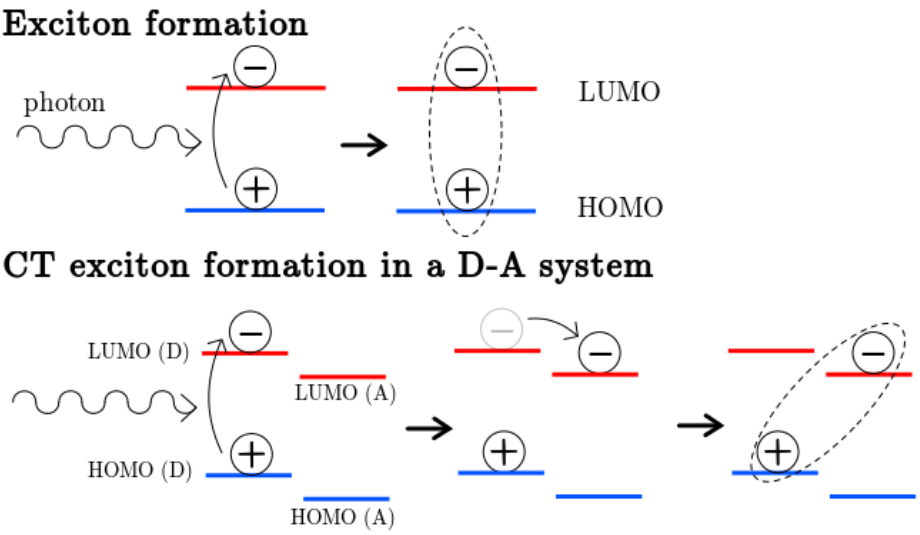

Figure 3: Schematic diagram of exciton formation, showing the difference between a CT exciton and one formed in the absence of an interface. [5, 1]

An excited electron in a material leaves behind a hole, which corresponds to a net positive charge. The electron and hole are attracted by the Coulomb force, and can form a bound state which resembles a hydrogen atom, known as an exciton. Normally, the spatial distance between the electron and hole is negligible or nonexistent, in which case the exciton has no dipole moment. However, in cases of a donor-acceptor (D-A) system, where an interface exists between two different molecules, the situation is complicated. It is possible to form an exciton where the electron and hole are spatially separated, located on different molecules (figure 3). This is known as a charge-transfer (CT) exciton.

CT excitons are particularly important for organic semiconductors because the low dielectric constants of organic materials means that charge separation tends to form CT excitons rather than free charges. Some force is then necessary to separate the hole and electron, such as an electric field applied over the sample. In the absence of an electric field to dissociate the exciton into free charge carriers, the exciton will typically decay on a timescale of <1 ns [1] (in our samples, the decay tended to take longer, on the order of a few nanoseconds at minimum).

CT exciton formation is helpful for current generation, because a CT state can aid in the

dissociation of an electron and hole. Specifically, when there is a wider spatial separation between the donor and acceptor, the exciton is bound more weakly (thanks to the $1/r^2$ dependence of the Coulomb force) and may contribute more easily to the generation of free charge carriers.

3 Methods

3.1 Sample preparation

Solutions were prepared at a concentration of ≈6 mM in toluene[1], with a 98-2% weight-weight mixture of donor and acceptor molecules respectively. These solutions were used to drop cast samples onto interdigitated electrode pairs, which were composed of 10 pairs of Cr/Au (5 nm / 50 nm layer thickness), each 25μm wide with 25μm gaps between them. Drop casting was done on a hot plate at 65 degrees C to ensure rapid evaporation of the solvent and to help control sample thickness.

3.2 Experimental setup

In ADT-TES-F composite samples, the initial rise and primary decay take place on the order of nanoseconds. To capture them, we used both a 300 Mhz Agilent oscilloscope (this was for longer timescales, on the order of tens of nanoseconds) and a 50 Ghz Tectronix Digital Sampling Oscilloscope (DSO) capable of accurately resolving the sub-nanosecond rise time of the signal pulse. For the DSO measurements, we also used a Centellax 3-stage broadband amplifier. A schematic diagram of the experimental setup is shown in figure 4. Labeled images of setup components are shown in figures 5 and 6.

The sample was excited by a pulsed 355 nm laser beam (Nd:YAG laser, 44.6 kHz), incident

[1]Later experiments, not discussed in depth in this thesis, have been conducted using chlorobenzene (CB) as the solvent. So far, results indicate that samples prepared using CB do not differ greatly, if at all, from the toluene-prepared samples. This is reasonable, given that the solvent evaporates when the samples are drop cast and should be almost completely gone by the time measurements are taken.

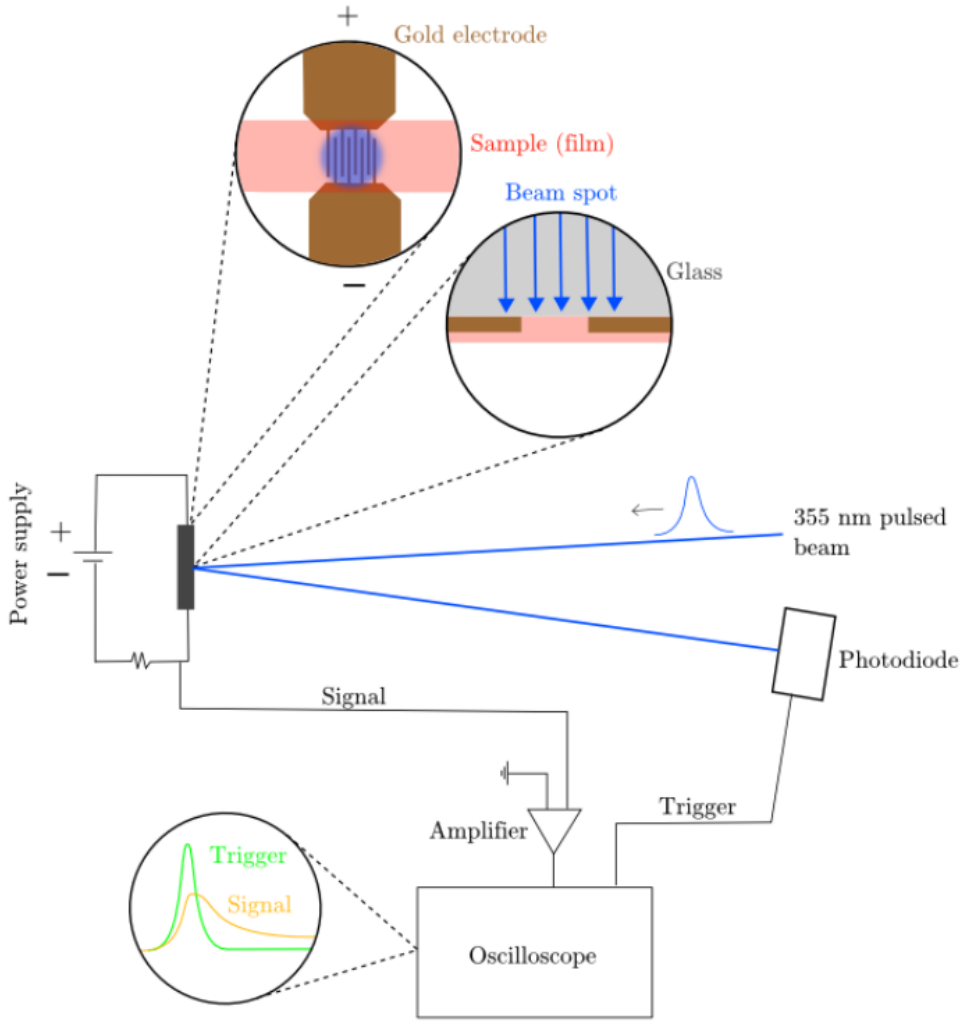

Figure 4: Experimental diagram for a transient photoconductivity experiment.

near normal on the film. The sample was back-illuminated so as to ensure the excitation of the material nearest the electrodes (an important consideration, given that most organic materials exhibit optical absorption depths on the order of 100 nm, [1] while drop-cast samples can be much thicker). The reflected beam was aligned into a photodiode, which detected the pulses and was connected to the trigger input of the oscilloscope. Each time a pulse registered on the trigger channel, the oscilloscope took a measurement. Meanwhile, voltage was applied over the sample and the resulting photocurrent was measured (by way of measuring the voltage over a resistor attached to the output of the sample holder). The

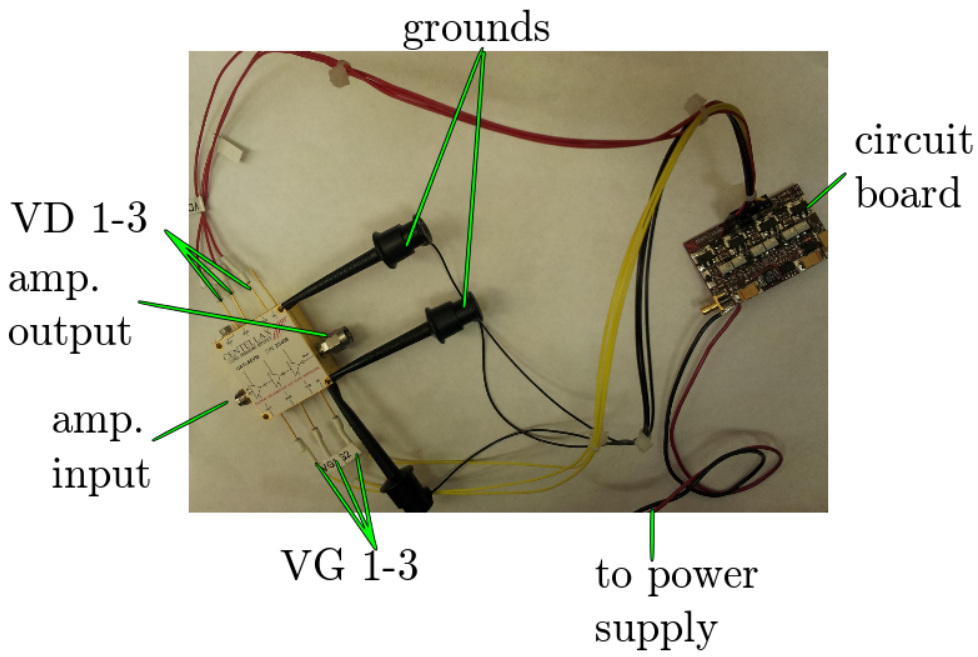

Figure 5: Experimental setup detail: amplifier circuit. (The precise workings of the circuit board are not important; it simply supplies power to the amplifier. The casing is grounded.)

signal from most samples was low, so the amplifier was used to boost the voltage entering the oscilloscope. By averaging over multiple measurements (generally 512 on the DSO), it was possible to get a reliable and reproducible measure of the transient photoconductivity signal.

3.3 Experimental issues of note

3.3.1 Pulse width and rise time

Investigation of the signal rise time was limited by the laser's pulse width, which is about 500 ps. For some trials, the observed signal rise time was well under 1 ns, meaning that the shape and duration of the pulse probably had a significant impact on its form. However, at low voltages on certain samples, (e.g. 20.V for IF-TCHS and IF-TIPS), the rise time was multiple nanoseconds long. We may therefore conclude that while the pulse width did limit investigation of the rise time, it did not erase all meaningful information in the comparison

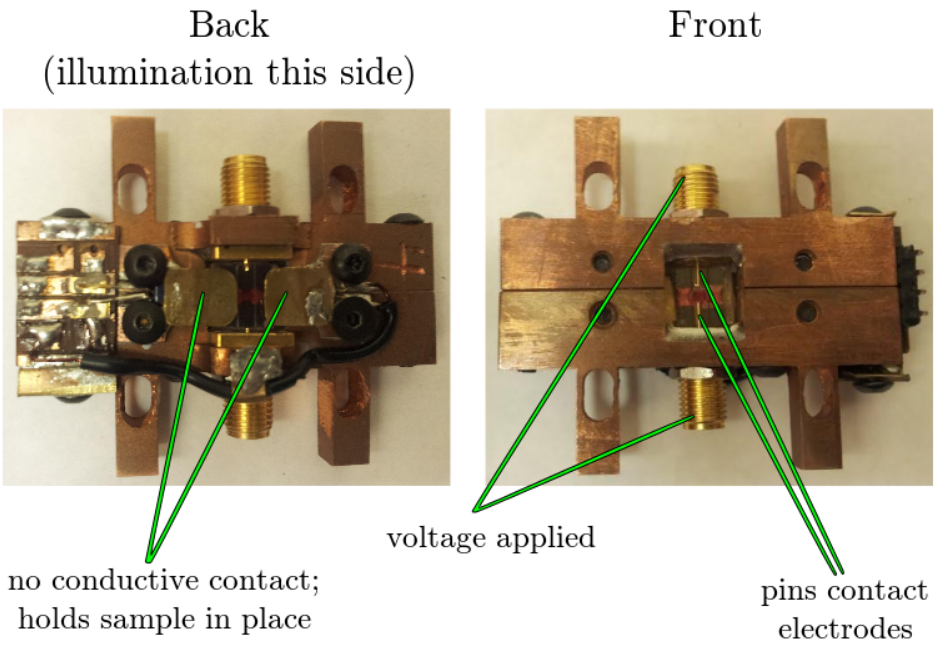

Figure 6: Experimental setup detail: sample holder. This photo shows the sample holder with a sample in place (the pink section between the pins is the TES-F composite itself, on electrodes).

of different samples and applied voltages. The Agilent oscilloscope could not clearly resolve the rise time at all; this was the fundamental reason for using the DSO for short-timescale measurements.

3.3.2 Unstable pulse train [2]

The pulse train was regularly checked for consistency using the Agilent oscilloscope over the course of the experiment. There was some instability in the train. Specifically, the laser occasionally produced an alternating train of higher and lower amplitude peaks (generally one was about 1/2 to 3/4 the height of the other). The instability made it difficult to properly set the trigger level (i.e. The voltage at which the oscilloscope would trigger and

[2]Pulse train stability, as measured from the trigger channel, was an important issue at the time that we were taking the data referenced in this thesis. Since then, we have moved from triggering on the reflected beam to triggering from a beam pick-off. We have also not recently had issues with the stability of the laser pulse train. Whether there is a causal connection here is unclear. In any case, I am including this section because it affected the data acquisition procedure at the time of the experiment.

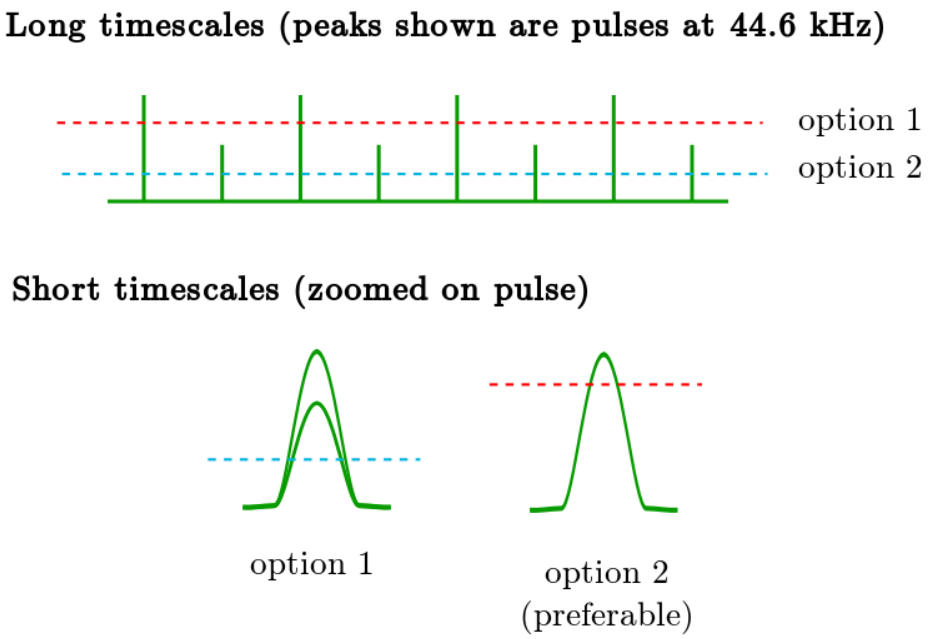

Figure 7: Diagram demonstrating the motivation for setting the trigger level between the two peak heights, given an unstable pulse train.

take a measurement). We decided to set the trigger level such that the oscilloscope would trigger only on the higher amplitude peaks (see figure 7 for a schematic diagram of this behavior). To do this, we set the trigger level between the two peaks whenever two were visible. The choice of trigger level meant that when the pulse train was unstable, every other pulse was not being recorded. This was acceptable because the duration between pulses was long enough (at 44.6 kHz) that the photocurrent decayed nearly to the level of the dark (non-illuminated) current before the next excitation. Furthermore, early calibration tests revealed that there was little difference between a trigger level which captured both peaks or just one, and it is possible that the careful trigger level choice was in fact unnecessary.

3.3.3 Sample degradation

Some of the samples degraded under illumination and applied voltage. Sample degradation could take one of several forms. First, it was possible to accidentally photobleach the samples (chemically damage them by over-exposing them to light). Second, high voltage and current

surges had the potential to damage the macroscopic structure of the sample, tearing away the film from the electrodes. This was especially true if the substrate had been improperly cleaned and treated before use, which would cause the film to bond poorly with the substrate (both the glass and the gold parts). We performed a series of tests which involved purposely exposing the samples to laser illumination and voltages over 200V, to determine exactly when this degradation began for each type of sample, and attempted to avoid any scenarios which caused sample damage in the future. Furthermore, all data was taken starting at low voltages, where the danger of sample damage was decreased, before moving to higher voltages. The lowest-voltage trials were repeated for comparison at the end of each round of data acquisition, to make sure that the high voltages had not damaged or destroyed the sample.

4 Results

In pristine donor films, the observed rise time of the photocurrent was limited by the resolution of the oscilloscope, which puts it under 0.6 ns. In donor-acceptor systems, however, some samples displayed a voltage-dependent rise time. Figure 8 (i) shows the results for the pentacene derivatives Pn-F8-TIPS and Pn-F8-TCHS. In the sample with the TIPS side-group, the photocurrent rise time was not dependent on the electric field, but in the TCHS sample, the slope of the initial rise increased with voltage. Figure 8 (ii) shows a similar trend between the indenofluorine derivatives, IF-TIPS and IF-TCHS. [3]

The data shown is normalized, because the peak photocurrent was dependent not only on the donor and acceptor but also on sample- or trial-specific factors (morphology of the film, precise alignment of the excitation beam, etc.), and also to facilitate comparison of the shapes of the curves. The faster rise time presumably corresponds to faster generation of charge carriers.

After the peak, the transient photoconductivity exhibited a two-stage decay. The first

[3]Further data can be found in the supplementary materials of [3].

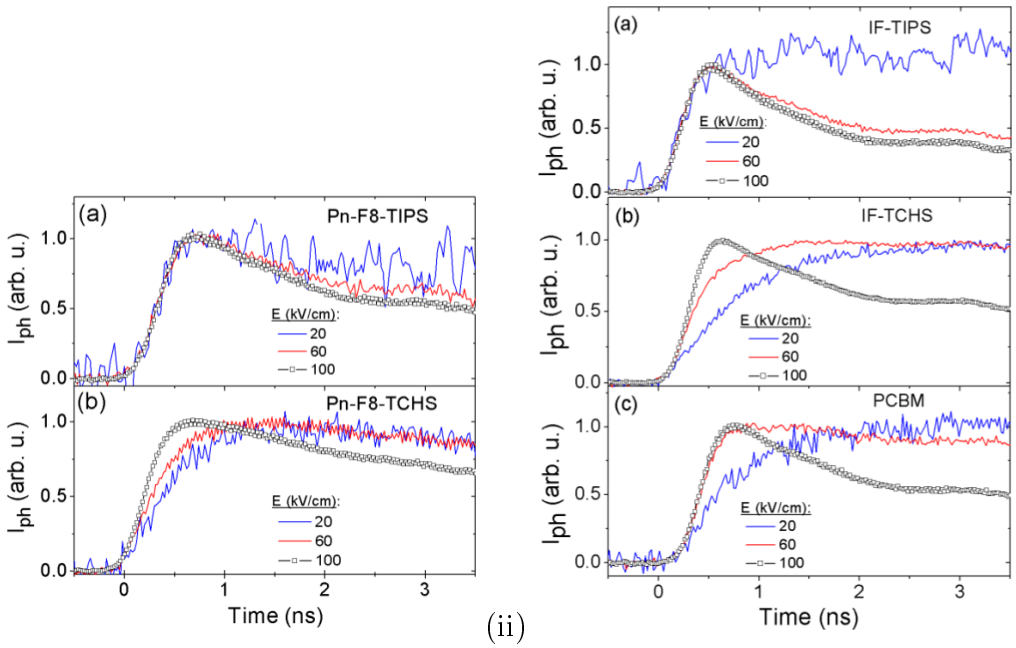

Figure 8: Rise time E-field (converted from applied voltage) dependence in D-A systems with different acceptors. These results are normalized at the photocurrent peak, to aid in shape comparison. Figures from [3].

stage was rapid, due to charge carriers recombining and being trapped in the material. This decay was dependent on the applied voltage, which is reasonable given that charge carrier mobility is expected to correlate with the electric field over the material. [4]

Note that our setup limited the rise-time resolution of samples with fast carrier generation, so these results do not imply that all TIPS-acceptor D-A systems have the same rise-time dynamics, but rather that any differences are only visible on the sub-0.6 ns timescale. The difference between samples with similar sidegroups can be seen in the post-peak decay shapes, which are E-field dependent and not uniquely determined by sidegroup (compare Pn-F8-TIPS with IF-TIPS at 20 kV/cm, for example.)

5 Discussion

Recall that the sidegroups of the donor and acceptor molecules affect their packing structure. Systems where the acceptor molecules have TIPS sidegroups are known to have a smaller

separation between the donor and acceptor, as opposed to those with other sidegroups (such as TCHS). In particular, there was a difference between systems with small D-A separations (TIPS acceptors) and those with large D-A separations.

In small-separation systems, a sub-0.6 ns rise time was observed, as with pristine films. But in large-separation systems, the rise time was dependent on applied voltage. Voltage dependence in the rise time indicates a larger contribution to the photocurrent by exciton dissociation, which makes sense given that the wider D-A separation is conducive to the dissociation of charge-transfer exciton states. Figure 8 (i.a, i.b, ii.a, ii.b) demonstrates this effect. Note that the rise time is not voltage dependent in the samples with acceptors with TIPS sidegroups, which correspond to more closely-spaced systems. The fast rise time in the TIPS acceptor samples is similar to that in pristine films.

Furthermore, we know from PL lifetime measurements (not discussed in this thesis; see [3]) that charge generation in these samples occurs faster than donor exciton dissociation, at all applied voltages. This indicates the presence of a precursor state which dissociates and contributes to the photocurrent. In the pristine donor films, and in films with small D-A separations (e.g. TIPS films), most of the photocurrent is due to this precursor state. It is only in samples with larger D-A separations that the dissociation of the CT exciton becomes important, and dominates over that of the precursor state.

Another interesting feature of the transient photocurrent measurements is that E-field dependent rise times were observed in samples where the PL measurements did not show evidence of a CT exciton state. Examples include the Hex-F8-TCHS, PCBM, and IF-TCHS composites. It is possible that, in these samples, there is a non-emissive CT state.

Besides the rise time measurements, it is worth noting some properties of the longer-timescale measurements. Most samples had a current decay which was split into two parts: a fast initial decay due to charge carrier trapping and recombination, and a slower secondary decay which followed a power law. In all samples studied, the initial decay was E-field dependent. This is most likely due to charge carrier mobility in the sample being E-field

dependent, [4] which would in turn lead to different trapping and recombination rates.

6 Conclusion

The rise-time results allow us to infer a rough picture of charge carrier dynamics within the sample. Immediately after excitation, a precursor state is formed. In pristine samples, this gives rise to a donor exciton and fast generation of charge carriers. In D-A systems, however, there is a competition process between the formation of donor excitons and charge transfer (CT) exciton states. CT exciton formation is followed by a relatively slow process of charge carrier generation via exciton dissociation. If the system has a wider D-A spatial separation, this CT state is more likely to make an important contribution to the photoconductivity. Because CT state dissociation is affected by the electric field applied, this mechanism accounts for the E-field dependence in large D-A separation systems as opposed to those with smaller D-A separations.

References

[1] Tracey M. Clarke and James R. Durrant. Charge photogeneration in organic solar cells. *Chemical Reviews*, 110(11):6736–6767, 2010.

[2] Stephen R. Forrest. The path to ubiquitous and low-cost organic electronic appliances on plastic. *Nature*, 428(6986):911–918, April 2004.

[3] M. J. Kendrick, A. Neunzert, M. M. Payne, B. Purushothaman, B. D. Rose, J. E. Anthony, M. M. Haley, and O. Ostroverkhova. Formation of the donor-acceptor charge-transfer exciton and its contribution to charge photogeneration and recombination in small-molecule bulk heterojunctions. *The Journal of Physical Chemistry C*, 116(34):18108–18116, 2012.

[4] A. D. Platt, M. J. Kendrick, M. Loth, J. E. Anthony, and O. Ostroverkhova. Temperature dependence of exciton and charge carrier dynamics in organic thin films. *Phys. Rev. B*, 84:235209, Dec 2011.

[5] X.-Y. Zhu, Q. Yang, and M. Muntwiler. Charge-transfer excitons at organic semiconductor surfaces and interfaces. *Accounts of Chemical Research*, 42(11):1779–1787, 2009. PMID: 19378979.

A Step-by-step calibration procedure using a GaAs standard

1. The experimental setup shown in figure4 has been slightly changed since the completion of the project described in this thesis. The trigger is no longer a reflection from the sample. Instead, a beam pick-off has been inserted near the laser which yields a trigger beam, a fraction the intensity of the excitation beam, and sends it directly to the photodiode through a fiber-optic cable. To begin the calibration procedure, connect the output of the photodiode to the Agilent oscilloscope and open the shutter on the laser. A pulse train should be visible on the oscilloscope.

2. Zoom the oscilloscope out to check the spacing of the pulse train. The 44.6 kHz frequency corresponds to a 22.4 μs spacing between pulses. Zoom in on the oscilloscope, and turn off the averaging, to check that the height of each pulse is constant. (If averaging is on, only one peak height will be visible even if the pulse height is not non-constant.) If the height of the pulses are unsteady, it will affect the choice of trigger level (section 3.3.2).

3. Make sure the maximum of the trigger signal pulse is below the input threshhold for the trigger port on the DSO (listed on the DSO itself). If it is not, change the alignment of the trigger pick-off until the signal is low enough to ensure that it will not overload the DSO. (Do not actually connect the trigger to the DSO yet.)

4. Set the trigger level on the Agilent at about 3/4 the height of the steady pulse (or see 3.3.2). Note the trigger level; it will need to entered into the DSO later.

5. Hook up the signal channel, without the amplifier, to the Agilent. Put the GaAs (gallium arsenide) reference in place and align the excitation beam between the electrodes. Check and note the power of the beam. Apply voltage (typically $\leq$ 5V is enough to see a clear signal from the GaAs) over the sample using the Keithley power supply.

Check to make sure the GaAs response is clearly visible and steady on the Agilent. This confirms that the trigger and signal channels are both working properly.

6. The goal is to produce a signal from the GaAs which can be used to test the experimental setup, including the DSO. Therefore, it is important that the DSO signal channel not be overloaded by the GaAs response. By adjusting voltage (and, if necessary, the power or alignment of the beam), tune the GaAs response well below $\frac{1}{\text{gain of the amplifier}} \times$ (threshhold of the DSO input). The effective gain for the Centellax amplifier, with a pulsed input signal, has been experimentally determined to be about 7. [4]

7. Shutter the beam. Connect the amplifier to the input of the Agilent. Connect the VG1-3 and VD1-3 wires to the pins and clip the grounds to the amplifier case, as shown in figure 5. Connect the wires to the circuit board. Power the circuit board with 10V from a power supply. It should draw 5.9 amps and all the LEDs on the circuit board should light up.

8. Open the shutter again, and check that the amplifier is properly amplifying the GaAs response. Confirm that:

   (a) the shape of the peak and decay are not significantly altered.

   (b) noise is within a tolerable level for the measurement you want to take.

   (c) the peak voltage will not overload the DSO.

   (d) the signal is being inverted through the amplifier.

9. Close the shutter, turn off the power to the amplifier, and transfer the amplifier to the input of the DSO. Be sure to include the DC block immediately after the amplifier; this will prevent any background current from overloading the DSO after it is amplified.

[4] The gain is actually frequency dependent. This is not a number from the device specifications, but a number pertaining to the actual height increase of the signal peak in our experiments, after amplification.

10. With the amplifier on and shutter open, check that the pulse is clearly visible on the DSO. If it is not, there may be an issue with the delay time between the trigger and signal channels. Increase or decrease the length of the trigger cable until the signal is visible.

If these steps are completed successfully, the setup should be ready to take data.

B Recent changes to the experimental setup

This thesis has described our lab's transient photoconductivity setup as it was at the time of data collection for the results shown. However, improvements have since been made to the apparatus. This appendix is included as a reference for the use of our current setup. Important changes are as follows:

- The trigger path. Previously, the pulse used to trigger the oscilloscope came from the reflection of the laser off the sample. Now, a mirror near the output of the laser picks off a small percentage of the beam's power, before it reaches the sample. This trigger signal is routed through a fiber optic cable directly to a photodiode. This has two major benefits: first, it means that the trigger beam can be directly coupled into the photodiode, and there is little need to worry about shielding the photodiode from the room lights. Second, it means that there is no need to align the beam into the photodiode each time a measurement is performed, which was a significant time sink before. The trigger path is now quite reliable and can be used with minimal adjustment across days or weeks.

- Pulse train stability. Although the reasons are not clear, since the setup was last disassembled and rebuilt, the issues described in section 3.3.2 seem to have disappeared. It is possible that what we read as an instability in the laser pulse train itself was somehow due to the reflection trigger path. Whatever the cause, it has not recently

been necessary to pay significant attention to the trigger level (although checking it regularly is still prudent).

- Drop-cast versus spin-cast films. The samples for this thesis were primary drop-cast, making them relatively thick and irregular in shape. Recently, we have begun using spin-cast films whenever possible, as they are far more regular. This allows for greater reproducibility between samples. However, the spin-cast films sometimes yield lower signal levels, and are often more difficult to use for PL measurements.